Spatial Model of Interferon Regulated Viral Infection on Two Dimensional Murine Lung Geometry

Benjamin Whipple

ABSTRACT

It is well understood that viral infections and the resulting immune response occur as a spatial process physiologically. Data limitations often guide modeling towards aggregated compartmental models rather than spatially explicit models of infection. Where spatial models of the dynamics have been considered, the considered domains are often restricted to simple uniform geometry. However, it is understood that the realized dynamics of a spatial process are dependent on the domain. Incorporation of both spatial dynamics and more realistic domains is crucial to improve the accuracy of predictions generated from in-silica models. As part of ongoing research, we extend a previously formulated model of within-host viral-immune dynamics to reconstructed lung geometry. Although further work is necessary to both improve the simulation performance and refine model parameter values, we see improvements in the dynamics from inclusion of more realistic spatial domains.

1 Introduction

Respiratory viral infections present a significant burden on global health. Seasonal influenza virus alone is estimated to cause on average over 350 thousand deaths annually, including in developed countries such as the United States[1,2]. Modeling of within-host viral infections, even if restricted to more accessible cases such as influenza, can enable and accelerate the development of effective treatments for related viral infections more generally[3].

Ordinary differential equations (ODE) are one of the most common methods to model within host infection dynamics[3]. Of the ODE models used to model within-host viral infections, the target cell model is one of oldest and most commonly considered[3–6]. While widely used, these ODE models adopt at least two assumptions common to compartmental models which are difficult to align with high fidelity modeling: that the interacting species are well mixed that the quantities are sufficiently large to assume a continuous approximation of the dynamics[7]. While the latter case is fundamental to pure differential equation models, the former can be solved by introducing spatial dimensions through partial differential equations (PDE)[7]. Due in part to both the increased computational complexity and increased difficulty of acquiring experimental data for spatial dynamics, spatial models are far less common in the context of within-host viral infection modeling. Most of the work incorporating spatial dynamics utilize one or two spatial dimensions under symmetry assumptions, or forego differential equation models for agent-based or cellular automata approaches[8–11]. It is acknowledged that the underlying topology of the infected space is likely significant in determining the course and outcome of the infection[8–11].

One manner in which the underlying infection topology is assumed to matter is in paracrine signalling within the immune system. Lavigne et al. (2021) exposit the possibility of "ring vaccination" based on an interferon response flowing from infected cells to suppress other infected cells and induce a resistant state in uninfected cells[9]. They find some evidence for this phenomena in by in-silica modeling using a single dimensional PDE and an agent-based model in three dimensions. While Levigne et al. a simple uniform spatial domain, it is clear that the spread of interferon, and the quarantining of infected cells, is highly dependent on the topology of the infected space. As an example, infections of the lung which do not proceed to viremia are constrained by the complex topology of the alveolar regions. This may contribute to better suppression by a "ring vaccination" phenomena than would be suggested by a simple uniform domain.

To further an ongoing investigation of the role that the underlying lung topology may play in severe respiratory infections we work to extend the model of Lavigne et al. (2021) to preliminary murine lung imaging data[9]. This proceeds by smoothing the point cloud data in order to enable simulation of a PDE. Then we extend the PDE system to two spatial dimensions and conduct an appropriate rescaling of the model parameters. Finally we implement and simulate of the system. While our preliminary results indicate that the model parameters need to be refined, the model trajectories take a biologically reasonable form compared to established patterns in influenza A virus dynamics.

2 Methods

2.1 Domain Reconstruction

Preliminary work by a colloborative lab has resulted in a two dimensional point cloud of cell nuclei within a mouse lung shown in Figure 1. The data was constructed by taking a 5 μm thick stained slice of mouse lung, photographing it under a microscope,

and then passing the photographs through various traditional and machine learning computer vision processes to highlight the nuclei of cells in the slide [1].

Figure 1 is a small region within the full image selected due to percieved nontrivial topology. We adopt the simplifying approximation that each pixel corresponds to a distinct cell nucleus. Following this interpretation, the full image contains nearly 170 thousand cells. In contrast, our test case contains about 2000 cells at about 1 percent of the total pixel area of the full image. We emphasize that this data remains highly approximate at this stage in the research.

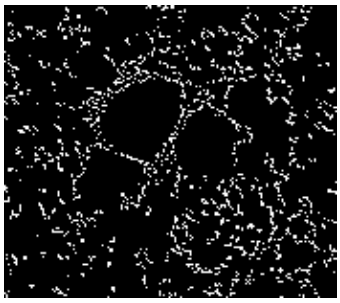

Figure 1. The considered domain.

We see in Figure 1 the suggestion of several topological features. The predominant features are three large holes in the center of the image. Smaller possible pockets are visible throughout the image, with differing clustering. This variability in topological structure suggests the possibility of more complex phenomena for spatial infection dynamics

Partial differential equations traditionally require a continuous underlying domain on which to simulate them. While point cloud data such as shown in Figure 1 clearly does not constitute such a domain, several methods can be used to extrapolate such a domain from it. One method consists of locally reconstructing an implied manifold through principal components and K-nearest neighbors[12]. Another approach involves lifting the data to the space of distributions by interpretting each point as a point mass δ_{x_i}, "blurring" the data using a compactly supported functional such as the bump function

$$\Psi(x;\varepsilon) = e^{-\frac{1}{1-(x_1^2+x_2^2)/\varepsilon^2}} 1_{\{\sqrt{x_1^2+x_2^2}/\varepsilon<1\}}.$$

We use this distribution blurring approach due to percieved advantages of relatively low computational complexity, relatively easy interpretation, and simple computer implementation[13].

Two important features of this approach are the partial preservation of topological properties and the approximate conservation of cell quantity. Given that $\Psi(x;\varepsilon)$ has compact support, then suitable choices of ε will connect the domain without removing holes and gaps. Further, by numerically computing a normalizing constant $C(\varepsilon)$ for $\Psi(x;\varepsilon)$, we can retain the interpretation of the total quantity of cells even after transforming the domain.

2.2 Mathematical Model

Our mathematical model is a two dimensional extension of the model from Lavigne et al. (2021)[9]. This model, presented in equation (1), describes the immune dynamics in a manner reminiscent to traditional target cell models[3,6]. We proceed to explain the components of the model.

Target cells T are infected by virus V at a rate β, converting them to infected cells I. Infected cells I produce virus V at a rate p as well as interferon F at a rate πp. Infected cells are cleared from the system at rate δ and enter an antiviral state I^* at rate k. Virus is cleared by the system at a rate c and diffuses through space with diffusion constant D_V. Interferon F interacts with infected cells I, accelerating their conversion to an anti-viral state I^* by rate ϕ, which have identical dynamics except that their production of virus V is reduced to $(1-f)p$. Interferon F also converts target cells T to a refractory state R at rate ϕ, providing temporary immunity from infection until converted back to T at rate ρ. Interferon also clears the system at rate c and diffuses with diffusion constant D_V. We omit the parameter values for sake of brevity and instead refer the interested reader to the related computer code.

$$\begin{aligned}
\partial T/\partial t &= -\beta VT - \phi FT + \rho R \\
\partial I/\partial t &= \beta VT - \delta I - kI - \phi FI \\
\partial I^*/\partial t &= kI + \phi FI - \delta I^* \\
\partial R/\partial t &= \phi FT - \rho R \\
\partial V/\partial t &= pI + (1-f)pI^* - cV + D_V\Delta V \\
\partial F/\partial t &= \pi p(I+I^*) - cF + D_F\Delta F
\end{aligned} \tag{1}$$

2.3 Numerical Methods

We simulate the previous system using the method of lines[14]. The method of lines involves discretizing the partial differential in space, transforming the original PDE into a large system of ODE with respect to time. We can then integrate the system using a traditional ODE solver, such as the 5th order Runga-Kutta method by Dormand and Prince[15]. Compared to classic finite difference approaches, this approach provides similar flexibility in determining the spatial discretization of our system while enabling us to rely on mature ODE solvers for temporal evolution of the system[14,16].

[1] Due to the nature of the ongoing collaboration we do not know the procedure in greater detail than described previously. This includes information such as the final scale of the image.

We utilize the blurred mask to determine initial conditions for the system. This determines the approximate quantity of target cells at each location in the domain. Given this domain, we select 5 initial points of infection and initialize a single infected cell at those locations.

We utilize the standard anisotropic discretization of the laplacian with masking to enforce internal no-flux boundary conditions. The general form of the basic laplacian ΔC is:

$$\Delta C = \frac{C_{i+1,j} - 2C_{i,j} + C_{i-1,j}}{dx^2} + \frac{C_{i,j+1} - 2C_{i,j} + C_{i,j-1}}{dy^2}.$$

The simulation requires no-flux boundary conditions on internal voids and along the external boundary of the space. We use a mask of the spatial locations of the voids and edge to zero out the discretized laplacian in those regions. This mask is determined from the blurred image.

2.4 Implementation Details

For our domain reconstruction we use smoothing parameter $\varepsilon = 7.5$. This code is contained in the file "Smoothing.py". Parameter ε is currently understood as a length dimension in number of pixels. The resulting field was sampled into a 100x100 grid and serialized as file "T0_map.txt".

Forward simulation of the model was conducted on GPU in file "Simulation.py". Forward simulation was conducted across the time span $t \in [0, 16]$ using a Dormand-Prince 5th order explicit Runga-Kutta method with adaptive time stepping. Other integration schemes were considered and while they were informally found to meaningfully differ in execution time, they had little effect on the resulting output.

All code was written in Python (version 3.10) using PyTorch (version 2.3) and TorchDiffeq (version 0.2.4) and is available on GitHub (link). PyTorch is most commonly used for research involving neural networks, but provides a simple method to differentiably program linear algebra intensive operations on GPU[17]. TorchDiffeq is a library implementing common ordinary differential integrators in PyTorch while enabling adjoint based differentiation through the solvers[18]. Forward simulation was conducted on an RTX 3090 GPU and took approximately 1 minute of runtime.

3 Results

Our preliminary results are presented across Figures 2, 3 and 4. Figure 2 depicts our domain reconstruction, showing the shift from the original point cloud, to a smoothed field with a connected but non-uniform domain. Figure 3 confirms that our simulation functions properly and that the topology of the domain introduces impacts the evolution of concentrations. Finally, Figure 4 depicts a broad agreement with expected dynamics from target-cell based models, with spatial complexity visible in the fluctuations around days 2 and 6. These figures broadly show that our method is effective at extending the viral-system to more accurate domain geometry.

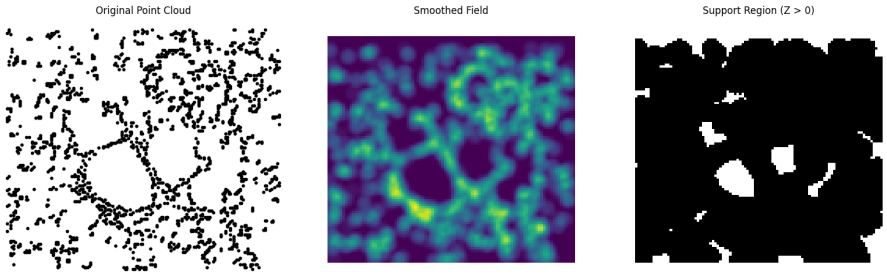

Figure 2. The reconstructed domain. The leftmost figure shows the original point cloud. The center figure shows the smoothed field, with brighter spots indicating higher cell concentrations. The rightmost figure shows the support region of the reconstructed domain with areas in black indicating the domain and areas in white indicating voids.

4 Discussion

We extend an existing PDE model of a model of interferon signalling and resistance target cell model to two spatial dimensions[9]. Using preliminary imaging data from a murine lung we are able to approximate 2D mouse lung topology for our simulation. Our use of smoothing on the point cloud data helps approximately resolve the conflict between continuum based dynamics with

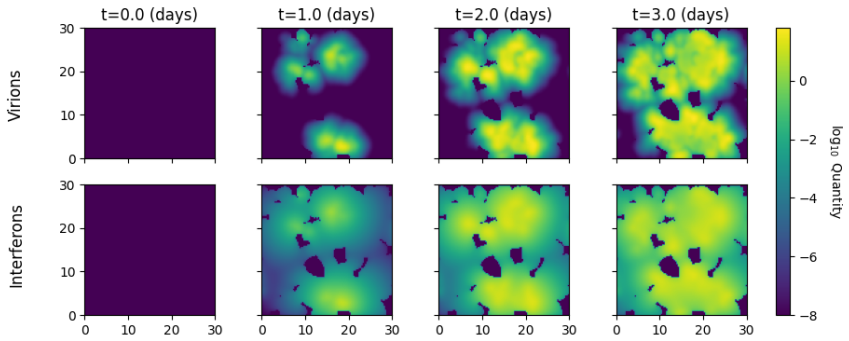

Figure 3. Virion and interferon concentrations across the first 3 days of simulation. We can see that the interferon response spreads more quickly across space than the virion concentration, as modeled in previous literature[9]. Further, we can see that the topology of the domain introduces impacts the evolution of concentration.

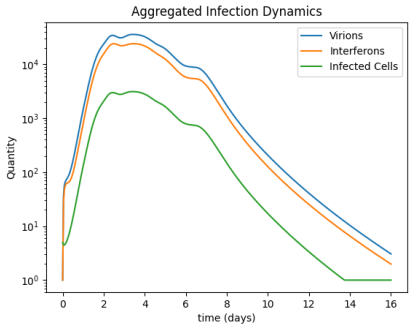

Figure 4. Aggregated dynamics for virions, interferons, and infected cells across space. As is typical with the target-cell related models of within host infection, there is exponential growth, a peak, and then decline within 15-20 days. The depicted states all appear highly correlated, which is also typical and expected from the given dynamics.

discrete biological features at high biological resolution. Finally, we see that the resulting simulations behave as expected from previous literature[3,6,9].

Several limitations and challenges remain to be addressed in future work. First, our model is relatively computationally expensive. Extensions to larger domains of the full images are significantly more burdensome computationally which will present difficulties to the application of common model analysis techniques in systems biology. As such, there is a need to improve the computational efficiency of the model as well as the distributability of the overall simulation.

Second, the model should be extended to incorporate additional or different aspects of the immune response. The model presented in equation (1) represents a dramatic simplification of the immune response which omits many known mechanisms of both the innate and adaptive immune response. Specific extensions will depend on experimental constraints and determined project aims, and so are as yet undetermined.

Third, the model parameter choices are relatively poorly grounded on the biological literature. This difficulty is present even with the original work where values are taken from multiple different experimental models[9]. While it is unlikely that the exact parameters needed for the model can be determined from the immunological literature, plausible bounds may be determined. Further analysis across this parameter space can be done to determine regions where different qualitative structures in the dynamics arise.

Finally, construction of a stochastic simulation algorithm approach should be done for comparison against our continuous dynamics[19]. These stochastic reaction models enable the consideration of discrete phenomena which is more accurate for distinct population elements than differential equation approaches. A stochastic reaction model would better capture discrete features of our simulation, such as distinguishable cells, although would require hybridization or dramatic computational resources to manage the large populations of virus and interferons. Development of such a model would provide a useful basis for comparison for our partial differential equation model.

References

1. Paget, J. *et al.* Global mortality associated with seasonal influenza epidemics: New burden estimates and predictors from the glamor project. *J. global health* **9**, 020421 (2019).
2. Zhou, H. *et al.* Hospitalizations associated with influenza and respiratory syncytial virus in the united states, 1993–2008. *Clin. infectious diseases* **54**, 1427–1436 (2012).
3. Boianelli, A. *et al.* Modeling influenza virus infection: a roadmap for influenza research. *Viruses* **7**, 5274–5304 (2015).
4. De Boer, R. J. & Perelson, A. S. Target cell limited and immune control models of hiv infection: a comparison. *J. theoretical Biol.* **190**, 201–214 (1998).
5. Baccam, P., Beauchemin, C., Macken, C. A., Hayden, F. G. & Perelson, A. S. Kinetics of influenza a virus infection in humans. *J. virology* **80**, 7590–7599 (2006).
6. Sachak-Patwa, R., Lafferty, E. I., Schmit, C. J., Thompson, R. N. & Byrne, H. M. A target-cell limited model can reproduce influenza infection dynamics in hosts with differing immune responses. *J. Theor. Biol.* **567**, 111491 (2023).
7. Das, J. & Jayaprakash, C. *Systems immunology: An introduction to modeling methods for scientists* (CRC Press, 2018).
8. Gallagher, M. E., Brooke, C. B., Ke, R. & Koelle, K. Causes and consequences of spatial within-host viral spread. *Viruses* **10**, 627 (2018).
9. Michael Lavigne, G., Russell, H., Sherry, B. & Ke, R. Autocrine and paracrine interferon signalling as 'ring vaccination'and 'contact tracing'strategies to suppress virus infection in a host. *Proc. Royal Soc. B* **288**, 20203002 (2021).
10. Moses, M. E. *et al.* Spatially distributed infection increases viral load in a computational model of sars-cov-2 lung infection. *PLoS computational biology* **17**, e1009735 (2021).
11. Quirouette, C., Younis, N. P., Reddy, M. B. & Beauchemin, C. A. A mathematical model describing the localization and spread of influenza a virus infection within the human respiratory tract. *PLoS computational biology* **16**, e1007705 (2020).
12. Liang, J. & Zhao, H. Solving partial differential equations on point clouds. *SIAM J. on Sci. Comput.* **35**, A1461–A1486 (2013).
13. Ohtake, Y., Belyaev, A. & Seidel, H.-P. A multi-scale approach to 3d scattered data interpolation with compactly supported basis functions. In *2003 Shape Modeling International.*, 153–161 (IEEE, 2003).
14. Schiesser, W. E. *The numerical method of lines: integration of partial differential equations* (Elsevier, 2012).
15. Dormand, J. R. & Prince, P. J. A family of embedded runge-kutta formulae. *J. computational applied mathematics* **6**, 19–26 (1980).
16. Hundsdorfer, W. & Verwer, J. G. *Numerical solution of time-dependent advection-diffusion-reaction equations*, vol. 33 (Springer Science & Business Media, 2007).
17. Team, P. Pytorch 2: Faster machine learning through dynamic python bytecode transformation and graph compilation, DOI: 10.1145/3620665.3640366 (2023).
18. Chen, R. T. Q., Rubanova, Y., Bettencourt, J. & Duvenaud, D. Neural ordinary differential equations. *Adv. Neural Inf. Process. Syst.* (2018).
19. Gillespie, D. T. Stochastic simulation of chemical kinetics. *Annu. Rev. Phys. Chem.* **58**, 35–55 (2007).